ELSEVIER

15 July 1995

OPTICS COMMUNICATIONS

Optics Communications 118 (1995) 250–254

Experimental determination of radiative-transition rates and quantum efficiencies in $Er^{3+}:YAlO_3$

M. Pollnau [1], E. Heumann, T. Danger, G. Huber

Institute of Laser-Physics, University of Hamburg, Jungiusstraße 11, D-20355 Hamburg, Germany

Received 11 January 1995

Abstract

A method for the measurement of radiative-transition rates in rare-earth-doped laser crystals with several metastable levels is presented. The excited-state absorption in $Er^{3+}:YAlO_3$ is measured in a pump- and probe-beam experiment. With this information the populations of the metastable levels $^4I_{13/2}$, $^4I_{11/2}$, and $^4S_{3/2}$ are derived. In combination with data of the relative fluorescence intensities and fluorescence-decay curves the radiative rates and quantum efficiencies of transitions from these levels are experimentally determined. The results are compared to data from a Judd–Ofelt analysis.

1. Introduction

Since the development of the first rare-earth-doped crystal lasers during the early 1960's there has been an enormous interest in the understanding of the processes that lead to population inversion and stimulated emission within the lasing ions. Intraionic processes such as ground-state absorption (GSA), excited-state absorption (ESA), fluorescence, and multiphonon decay as well as interionic processes such as energy transfer, up-conversion, and cross relaxation have been identified to be the dominant population mechanisms of the laser levels.

The only parameters, however, that are directly accessible to experiments are the GSA and ESA cross sections. Another measured parameter, the inverse fluorescence-decay time of a level, represents a complicated sum of all contributing excitation and relaxation rates of this level. In general, it may depend on the pump level and the pump energy of the excitation as well as on the dopant concentration of the crystal. Owing to the lack of experimental information, theories and models have been introduced in order to determine the contributing parameters. With the Judd–Ofelt theory [1,2] the radiative-transition rates are calculated. Other models investigate the quantities of multiphonon transitions [3] and the transition probabilities of interionic processes [4]. The obtained data have as yet been verified by experimental results only for a few simple cases, but with questionable accuracy, because the exact measurement of quantum efficiencies is very difficult.

In this paper a method is presented that allows the experimental determination of radiative-transition rates in rare-earth-doped laser crystals with several metastable levels. Based on the knowledge of ESA cross sections [5] the absolute population densities of the metastable levels $^4I_{13/2}$, $^4I_{11/2}$, and $^4S_{3/2}$ in $Er^{3+}:YAlO_3$, see Fig. 1, are obtained from cw-pumped ESA experiments. Measurements of the relative fluorescence intensities under the same pump conditions

[1] Present address: Institute of Applied Physics, University of Bern, Sidlerstrasse 5, CH-3012 Bern, Switzerland.

SSDI 0030-4018(95)00225-1

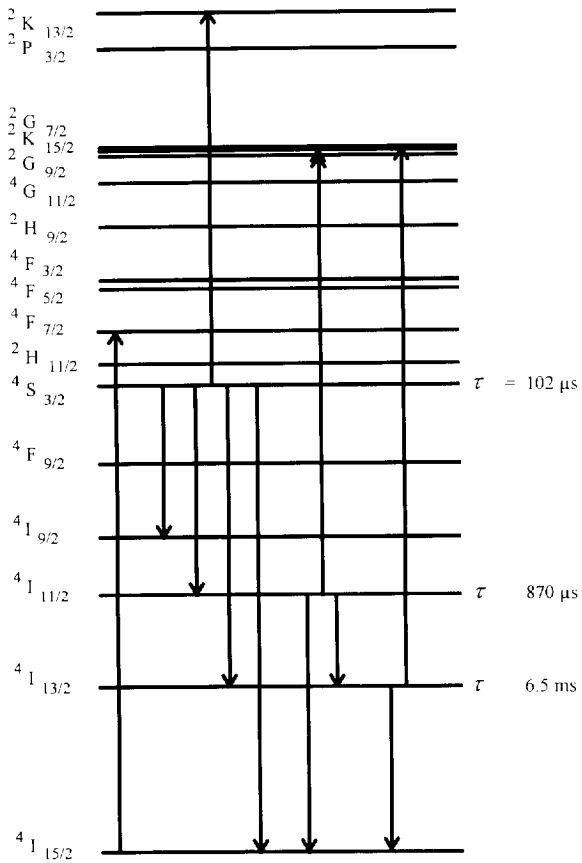

Fig. 1. Energy level scheme of $Er^{3+}:YAlO_3$ indicating excitation at 488 nm, detected fluorescence lines and largest ESA transitions from the metastable levels $^4I_{13/2}$, $^4I_{11/2}$, and $^4S_{3/2}$.

then lead to the determination of the relative radiative-transition rates originating form the metastable levels are derived because one radiative rate from one of these levels is known. The results are compared to data obtained from a Judd–Ofelt analysis [6,7]. With the measured fluorescence-decay curves, the quantum efficiencies of the system are derived from the experimental data.

Measurements of the absolute fluorescence intensities have been used so far for the determination of radiative-transition rates and quantum efficiencies. With this method the detector response as well as the geometrical arrangement of the detection are critical sources for experimental errors. This approach is especially critical in systems with various metastable levels because the quantum efficiencies of each level must be measured separately in a wide spectral range. Therefore, absolute fluorescence measurements have, to our knowledge, as yet not been applied to erbium-doped systems. The distinct advantage of our method is the fact that in the ESA as well as in the fluorescence measurements only relative intensities have to be detected and geometrical factors do not influence the results.

2. Experimental arrangements

A pump- and probe-beam technique is used for the measurement of cw-pumped ESA spectra, see Fig. 2. The $Er^{3+}(2.9\times10^{20}\ cm^{-3}):YAlO_3$ crystal (length $d=9.6$ mm, crystallographic a-axis) is placed between two pinholes of 200 μm in diameter in order to define the excitation volume. An Ar^+ laser with 250 mW at 488 nm excites the sample via mirror 1. The transmitted pump light passes through a hole in mirror 2. Pump light scattered into the direction of the monochromator is blocked by a filter or a diaphragm. A chopper frequency 1 Hz and duty-cycle 1:1 provides the trigger signal for the probe beam and interrupts the Ar^+ beam for the detection of the unpumped probe-beam spectra. Pulsed probe light from a broadband xenon flashlamp is focused into the sample via mirror 2. The transmitted probe-light spectrum passes through a hole in mirror 1, is analyzed by a monochromator (1/4 m spectrometer with grating 300 L/mm, resolution 3 nm) and is detected by a gated optical multichannel analyzer

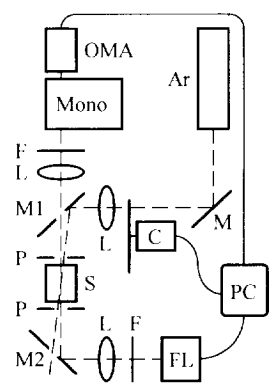

Fig. 2. Experimental arrangement for cw ESA measurements. $Ar=Ar^{+3}$ laser, C = chopper, F = filter, FL = flashlamp, L = lens, Mi = mirror i, Mono = monochromator, OMA = optical multichannel analyzer, P = pinhole, PC = personal computer and electronics, S = sample.

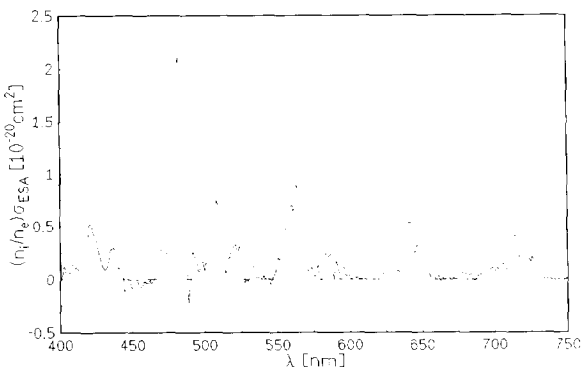

Fig. 3. cw-pumped ESA spectrum of Er^{3+} (2.9×10^{20} cm^{-3}) : $YAlO_3$. The values of the largest transitions from the $^4I_{13/2}$, $^4I_{11/2}$, and $^4S_{3/2}$ levels are used to determine the population densities of the corresponding initial levels.

(OMA). The measurement of four spectra (application of no beam, pump beam, probe beam, pump and probe beam) results in a spectrum, which is free of scattered pump light and spontaneous fluorescence form the sample [5,8]. The cw ESA spectrum of $Er^{3+}:YAlO_3$ is shown in Fig. 3. Experimental results are given in Table 1.

For the measurement of the relative fluorescence intensities the sample is excited by an Ar^+ laser under the same conditions. The fluorescence signals are spectrally analyzed by a monochromator and detected by a S1 photomultiplier (visible range) or an InSb detector (infrared range), both cooled to liquid-nitrogen temperature. The spectral resolutions are 0.08 nm (S1, grating 1200 L/mm, 500 nm blaze) and 12.8 nm (InSb, grating 300 L/mm, 2 μm blaze), respectively. The pump light and higher orders of shorter-wavelength fluorescences are blocked by suitable edge filters. A lock-in technique is used for the improvement of the signal-to-noise ratio. The spectra are calibrated with a tungsten lamp at temperature 2600 K, whose spectrum is compared to the Planck curve at the same temperature. The 970 nm fluorescence is detected in the visible and infrared setup. The relative visible and infrared fluorescence intensities which are calculated in relative photon rates are normalized to this 970 nm fluorescence. Experimental results are given in Table 2.

The fluorescence-decay curve at 1.55 μm from $^4I_{13/2}$ is recorded by an InSb detector with chopped excitation by an Ar^+ laser at 488 nm. The curves are summed on a storage oscilloscope. The decay curves at 550 nm from $^4S_{3/2}$ and 970 nm from $^4I_{11/2}$ are monitored with a single-photon-counting technique by a S1 photomultiplier connected to a multichannel analyzer, after pulsed excitation by a N_2-laser-pumped dye laser (Coumarin 102) at 488 nm with 10 ns pulse duration. The measured lifetimes are given in Table 2.

3. Determination of radiative-transition rates and quantum efficiencies

In this section the evaluation of the radiative-transition rates and quantum efficiencies from the experimental data is described. Firstly the population densities of the metastable levels are calculated from the ESA experiments. Secondly the relative radiative-transition rates and, with the knowledge of one absolute rate, the absolute radiative-transition rates from these levels are determined from the relative fluorescence intensities. Finally the quantum efficiencies of the system are calculated from the measured lifetimes.

From the ESA experiments the population densities of the metastable levels are derived. n is the dopant concentration. $n_e = \sum_i n_i$ is the excitation density. The sum extends over all metastable and substantially populated levels i. $Er^{3+}:YAlO_3$ the $^4I_{13/2}$, $^4I_{11/2}$, and $^4S_{3/2}$ levels are contributing, see Fig. 1. In the ESA

Table 1
Investigated ESA transitions (cf. Fig. 1), measured data of ESA cross sections $\sigma_{ESA,i}$ times the relative excited-state population densities n_i/n_e under cw excitation (cf. Fig. 3), absolute ESA cross sections $\sigma_{ESA,i}$ [5], and population densities n_i calculated from the experimental data. The excitation density is $n_e = 2.9\times10^{18}$ cm^{-3}

Initial level i	terminating level	$\sigma_{ESA,i}$ [nm]	$(n_i/n_e)\sigma_{ESA,i}$ [10^{-20} cm^2]	$\sigma_{ESA,i}$ [10^{-20} cm^2]	n_i [10^{18} cm^{-3}]
$^4S_{3/2}$	$^2K_{13/2}$	677	0.04	1.6	0.09
$^4I_{11/2}$	$^2G_{7/2}$	564	0.9	2.6	1.0
$^4I_{13/2}$	$^2K_{15/2}+{}^2G_{9/2}$	482	2.1	5.1	1.2

Table 2
Investigated fluorescence transitions (cf. Fig. 1), measured fluorescence intensities I_{ij} relative to the $^4I_{11/2}$ ground-state fluorescence at 960–1030 nm, experimentally determined radiative-transition rates A_{ij} compared to values derived from Judd–Ofelt theory [6,7], measured lifetimes τ_i, and quantum efficiencies η_{ij} calculated from the experimental data

Initial level i	Terminating level j	$\lambda_{fluoresc}$ [nm]	I_{ij} [a.u.]	A_{ij} [s^{-1}]		τ_i [μs]	η_{ij} [%]
				exper.	theory		
$^4S_{3/2}$	$^4I_{15/2}$	540– 560	1347	897	1410 [a]	102	9.1
	$^4I_{13/2}$	840– 870	429	285	557 [a]		2.9
	$^4I_{11/2}$	1220–1250	39	26	51 [a]		0.3
	$^4I_{9/2}$	1640–1760	156	104	107 [a]		1.1
$^4I_{11/2}$	$^4I_{15/2}$	930–1030	1000	60	82 [b]	870	5.2
	$^4I_{13/2}$	2630–2930	492	30	31 [b]		2.6
$^4I_{13/2}$	$^4I_{15/2}$	1450–1650	3083	154	200 [b]	6500	100

[a] Ref. [6].
[b] Ref. [7].

arrangement the probe beam has a low intensity I_0 compared to the pump beam, such that the laser-induced populations of the levels are unperturbed. The transmitted probe-beam intensity I_p after laser excitation and I_u without excitation as well as the cross section σ_{GSA} are measured. With the equations for the transmission in the unpumped and pumped case,

$$I_u = I_0 \exp(-n\sigma_{GSA} d) , \tag{1}$$

$$I_p = I_0 \exp\left[-\left((n - n_c)\sigma_{GSA} + \sum_i n_i \sigma_{ESA,i} \right) d \right] , \tag{2}$$

the equation for the calculation of the ESA cross section $\sigma_{ESA,i}$ of the detected transition from initial level i at wavelength λ times the relative population density n_i/n_c of the initial level is derived [9]:

$$\frac{1}{dn_c} \ln \frac{I_u}{I_p} + \sigma_{GSA} = \sum_i \frac{n_i}{n_c} \sigma_{ESA,i} . \tag{3}$$

n_c is determined from the bleaching of the GSA in the $\ln(I_u/I_p)$ spectrum at wavelength regions where no ESA occurs, because at these wavelengths the right-hand side in (3) equals zero. The cross sections $\sigma_{ESA,i}$ were determined from time-resolved ESA measurements [5]. These measurements allow the experimental separation of the time-dependent excited-state population densities n_i from the constant cross sections $\sigma_{ESA,i}$ [9] and the calculation of both quantities under the conditions fo the time-resolved experiments. The cross sections remain the same under any pump condition and are used for the present evaluation. Thus the excited-state population densities n_i under cw excitation are calculated from (3). Experimental results are given in Table 1.

Now the radiative-transition rates are calculated from the fluorescence measurements. The relative fluorescence intensity I_{ij} of the detected transition from initial level i to terminating level j is proportional to the radiative-transition rate A_{ij} and the population density n_i of the initial level, i.e.

$$I_{ij} = CA_{ij} n_i . \tag{4}$$

Due to the calibration and the same geometrical conditions of the detection the constant C is identical for all fluorescences. Since the quantities I_{ij} and n_i have been determined the radiative-transition rates A_{ij} can be calculated relative to each other. In erbium-doped crystals the ground-state fluorescence from the $^4I_{13/2}$ level at 1.55 μm has no competing multiphonon transition because of its large energy gap. The inverse fluorescence lifetime τ_1^{-1} at 1.55 μm is thus identical to the radiative-transition rate A_{10}. This allows the determination of the constant C in (4). Now the absolute values of the other radiative-transition rates A_{ij} can be calculated from (4). Experimental results for the radiative-transition rates A_{ij} are given in Table 2.

With the fluorescence lifetime τ_i the quantum efficiencies η_{ij} of the radiative transitions from level i are obtained:

$$\eta_{ij} = A_{ij} / \tau_i^{-1} . \tag{5}$$

Experimental results for the quantum efficiencies η_{ij} are given in Table 2.

The experimental errors are 20% for the ESA data ($^4I_{13/2}$ and $^4I_{11/2}$), 10% for the fluorescence data, and 10% for the lifetime data. Owing to its relatively short lifetime the population density of the $^4S_{3/2}$ level is weak under cw excitation and only the strongest ESA transition at 677 nm could be detected as a small peak, see Fig. 3. The uncertainty of its magnitude and hence the uncertainty of the population density of the $^4S_{3/2}$ level is approximately 50%. Improvements in the ESA arrangement — especially the reliability of the excitation pulse in the time-resolved arrangement [5] and a higher sensitivity of the OMA detection system — will lead to more accurate results.

4. Comparison to Judd–Ofelt analysis

The experimental values for the radiative-transition rates are compared to data derived from a Judd–Ofelt analysis [6,7], see Table 2. The results for the transitions from $^4S_{3/2}$ show a significant difference of up to 50% for some rates due to the experimental uncertainty mentioned above. The result for the transition $^4I_{11/2} \rightarrow {}^4I_{13/2}$ is in good agreement with theory. Deviations of approximately 30% must be attributed to the Judd–Ofelt results due to the simplifications of the theory, such as the neglect of the Stark splitting of the levels and the assumption of an infinite temperature of the system. Especially the strong Stark splitting of the erbium ground state leads to errors if this level is treated as a single state [10]. For example the Judd–Ofelt rate for A_{10} should equal the measured inverse lifetime of 154 s^{-1} or it should be smaller if nonradiative channels contribute to the decay of the $^4I_{13/2}$ level. Instead the theoretical value is higher. For the same reason the theoretical value of the transition $^4I_{11/2} \rightarrow {}^4I_{15/2}$ is too large.

5. Conclusions

A method for the experimental determination of radiation-transition rates in rare-earth-doped laser crystals with several metastable levels has been demonstrated. The excited-state-absorption, relative-fluorescence-intensity, and lifetime data of $Er^{3+}:YAlO_3$ have been measured and the relative radiative-transition rates have been determined. With the knowledge of the rate from the $^4I_{13/2}$ to the $^4I_{15/2}$ level the absolute values of all other radiative-transition rates are obtained. The comparison to Judd–Ofelt data shows significant differences which can be attributed to deviations in both, experiments and theory. The quantum efficiencies of the system are obtained from the experimental results.

Acknowledgements

The authors thank H. Stange and R. Groß of the Institute of Laser-Physics, University of Hamburg, Germany, for the development of parts of the experimental arrangements and for many helpful discussions. This work was supported by the Deutsche Forschungsgemeinschaft.

References

[1] B.R. Judd, Phys. Rev. 127 (1962) 750.
[2] G.S. Ofelt, J. Chem. Phys. 37 (1962) 511.
[3] L.A. Riseberg, W.B. Ganrud and H.W. Moos, Phys. Rev. 159 (1967) 262.
[4] D.L. Dexter, J. Chem. Phys. 21 (1953) 836.
[5] M. Pollnau, E. Heumann and G. Huber, Appl. Phys. A 54 (1992) 404.
[6] R. Reisfeld and C.K. Jørgensen, Lasers and excited states of rare earths, eds. M. Becke, M.F. Lappert, J.L. Margrave, R.W. Parry, C.K. Jørgensen, S.J. Lippard, K. Niedenzu and H. Yamatera, 1st Ed. (Springer, Heidelberg, 1977).
[7] P.A. Arsenjew et al., Kristalle in der modernen Lasertechnik, ed. P. Görlich (Akademische Verlaggesellschaft, Leipzig, 1980).
[8] S.A. Payne, L.L. Chase and G.D. Wilke, Phys. Rev. B 37 (1988) 998.
[9] M. Pollnau, E. Heumann and G. Huber, Phys. Status Solidi A 130 (1992) K121.
[10] S. Georgescu, C. Ionescu, I. Voicu and V.I. Zehkov, Rev. Roum. Phys. 30 (1985) 265.